

Highlights from Fermi GRB observations

JONATHAN GRANOT

on behalf of the Fermi LAT and GBM collaborations

Centre for Astrophysics Research, University of Hertfordshire,
College Lane, Hatfield AL10 9AB, UK

Abstract

The Fermi Gamma-Ray Space Telescope has more than doubled the number of Gamma-Ray Bursts (GRBs) detected above 100 MeV within its first year of operation. Thanks to the very wide energy range covered by Fermi's Gamma-ray Burst Monitor (GBM; 8 keV to 40 MeV) and Large Area Telescope (LAT; 25 MeV to > 300 GeV) it has measured the prompt GRB emission spectrum over an unprecedentedly large energy range (from ~ 8 keV to ~ 30 GeV). Here I briefly outline some highlights from Fermi GRB observations during its first ~ 1.5 yr of operation, focusing on the prompt emission phase. Interesting new observations are discussed along with some of their possible implications, including: (i) What can we learn from the Fermi-LAT GRB detection rate, (ii) A limit on the variation of the speed of light with photon energy (for the first time beyond the Planck scale for a linear energy dependence from direct time of arrival measurements), (iii) Lower-limits on the bulk Lorentz factor of the GRB outflow (of ~ 1000 for the brightest Fermi LAT GRBs), (iv) The detection (or in other cases, lack thereof) of a distinct spectral component at high (and sometimes also at low) energies, and possible implications for the prompt GRB emission mechanism, (v) The later onset (and longer duration) of the high-energy emission (> 100 MeV), compared to the low-energy ($\lesssim 1$ MeV) emission, that is seen in most Fermi-LAT GRBs.

1 Pre-Fermi high-energy GRB observations

The Energetic Gamma-Ray Experiment Telescope (EGRET) on-board the Compton Gamma-Ray Observatory (CGRO; 1991–2000) was the first to detect high-energy emission from GRBs. EGRET detected only five GRBs with its Spark Chambers (20 MeV to 30 GeV) and a few GRBs with its Total Absorption Shower Counter (TASC; 1 – 200 MeV). Nevertheless,

these events already showed diversity. The most prominent examples are GRB 940217, with high-energy emission lasting up to ~ 1.5 hr after the GRB including an 18 GeV photon after ~ 1.3 hr, [1] and GRB 941017 which had a distinct high-energy spectral component [2] detected up to ~ 200 MeV with $\nu F_\nu \propto \nu$. This high-energy spectral component had ~ 3 times more energy and lasted longer (~ 200 s) than the low-energy (hard X-ray to soft gamma-ray) spectral component (which lasted several tens of seconds), and may be naturally explained as inverse-Compton emission from the forward-reverse shock system that is formed as the ultra-relativistic GRB outflow is decelerated by the external medium [3, 4]. Nevertheless, better data are needed in order to determine the origin of such high-energy spectral components more conclusively. The Italian experiment Astro-rivelatore Gamma a Immagini LEggero (AGILE; launched in 2007) has detected GRB 080514B at energies up to ~ 300 MeV, and the high-energy emission lasted longer (> 13 s) than the low-energy emission (~ 7 s) [5]. Below are some highlights of Fermi GRB observations so far and what they have taught us.

2 LAT GRB detection rate: what can it teach us?

During its first 1.5 yr of routine operation, from Aug. 2008 to Jan. 2010, the LAT has detected 14 GRBs, corresponding to a detection rate of $\sim 9.3 \text{ yr}^{-1}$. Table 1 summarizes their main properties. While at least 13 of the 14 LAT GRBs had ≥ 10 photons above 100 MeV, 4 were particularly bright in the LAT with ≥ 1 photon above 10 GeV, ≥ 10 photons above 1 GeV, and ≥ 100 photons above 100 MeV. This corresponds to a bright LAT GRB (as defined above) detection rate of ~ 2.7 GRB/yr (with a rather large uncertainty due to the small number statistics). There were also 11 GRBs with ≥ 1 photon above 1 GeV, corresponding to ~ 7.3 GRB/yr. These detection rates are compatible with pre-launch expectations [6] based on a sample of bright BATSE GRBs for which the fit to a Band spectrum over the BATSE energy range (20 keV to 2 MeV) was extrapolated into the LAT energy range (see Fig. 1). The agreement is slightly better when excluding cases with a rising νF_ν spectrum at high energies (i.e. a high-energy photon index $\beta > -2$).¹ This suggests that, on average, there is no significant excess or deficit of high-energy emission in the LAT energy range relative to such an extrapolation from lower energies. As described in § 5, however, in individual cases we do have evidence for such an excess. The observed LAT

¹Such a hard high-energy photon index may be an artifact of the limited energy range of the fit to BATSE data, or may be affected by poor photon statistics at $\gtrsim 1$ MeV.

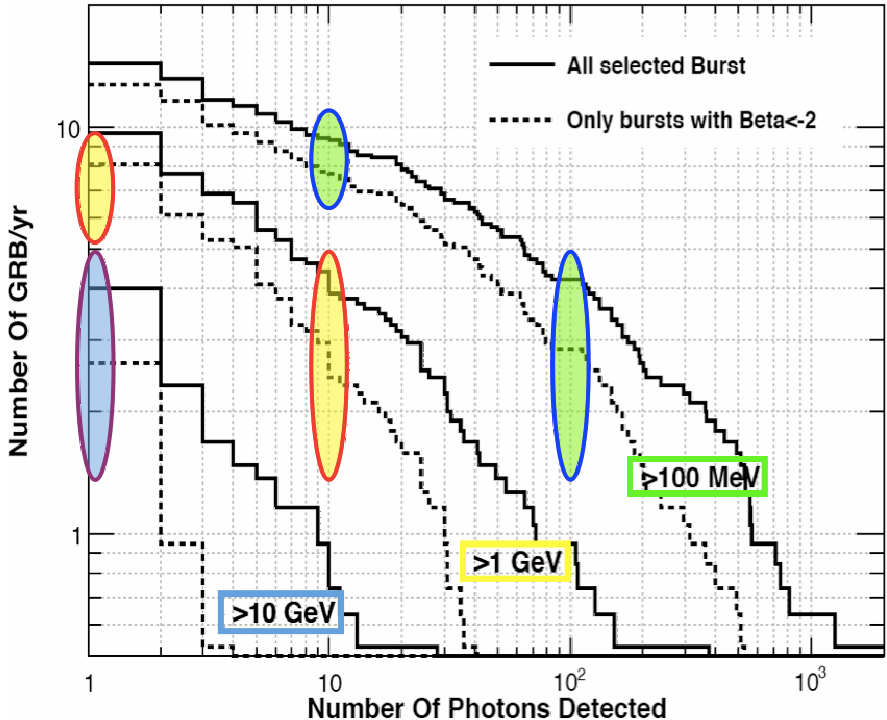


Figure 1: LAT GRB detection rates (color ellipses) superposed on top of pre-launch expected rates based on the extrapolation of a Band spectrum fit from the BATSE energy range [6]. The ellipses' inner color indicates the minimal photon energy (green, yellow and cyan correspond to 0.1, 1 and 10 GeV, respectively), while their height indicates the uncertainty ($\pm N^{1/2}/1.5$ yr) on the corresponding LAT detection rate ($N/1.5$ yr) due to the small number (N) of detected GRBs.

GRB detection rate implies that, on average, only about $\sim 10 - 20\%$ of the energy that is radiated during the prompt GRB emission phase is channeled into the LAT energy range, suggesting that in most GRBs the high-energy radiative output does not significantly affect the total energy budget. Short GRBs, however, appear to be different in this respect (see § 7 and Fig. 3).

3 Limits on Lorentz Invariance Violation

Some quantum gravity models allow violation of Lorentz invariance, and in particular allow the photon propagation speed, v_{ph} , to depend on its energy, E_{ph} : $v_{\text{ph}}(E_{\text{ph}}) \neq c$, where $c \equiv \lim_{E_{\text{ph}} \rightarrow 0} v_{\text{ph}}(E_{\text{ph}})$. The Lorentz invariance violating (LIV) part in the dependence of the photon momentum, p_{ph} , on

GRB	θ_{LAT}	long or short	number of events above		HE emission		extra spec. comp.	highest energy (GeV)	z
			0.1 GeV	1 GeV	starts	lasts			
					later	longer			
080825C	$\sim 60^\circ$	long	~ 10	0	?	yes	no	~ 0.6	—
080916C	49°	long	145	14	yes	yes	?	~ 13	~ 4.35
081024B	21°	short	~ 10	2	yes	yes	?	~ 3	—
081215A	$\sim 86^\circ$	long	—	—	?	?	—	—	—
090217	$\sim 34^\circ$	long	~ 10	0	no	no	no	~ 1	—
090323	$\sim 55^\circ$	long	~ 20	> 0	?	yes	?	?	3.57
090328	$\sim 64^\circ$	long	~ 20	> 0	?	yes	?	?	0.736
090510	$\sim 14^\circ$	short	> 150	> 20	yes	yes	yes	~ 31	0.903
090626	$\sim 15^\circ$	long	~ 20	> 0	?	yes	?	?	—
090902B	51°	long	> 200	> 30	yes	yes	yes	~ 33	1.822
090926	$\sim 52^\circ$	long	> 150	> 50	yes	yes	yes	~ 20	2.1062
091003A	$\sim 13^\circ$	long	~ 20	> 0	?	?	?	?	0.8969
091031	$\sim 22^\circ$	long	~ 20	> 0	?	?	?	~ 1.2	—
100116A	$\sim 29^\circ$	long	~ 10	3	?	?	?	~ 2.2	—

Table 1: Summary of the 14 GRBs detected by the LAT between August 2008 and January 2010 – its first 1.5 years of routine operation following Fermi’s launch on 11 June 2008; θ_{LAT} is the angle from the LAT boresight at the time of the GBM GRB trigger.

its energy, E_{ph} , can be expressed as a power series,

$$\frac{p_{\text{ph}}^2 c^2}{E_{\text{ph}}^2} - 1 = \sum_{k=1}^{\infty} s_k \left(\frac{E_{\text{ph}}}{M_{\text{QG},k} c^2} \right)^k, \quad (1)$$

in the ratio of E_{ph} and a typical energy scale $M_{\text{QG},k} c^2$ for the k^{th} order, which is expected to be up to the order of the Planck scale, $M_{\text{Planck}} = (\hbar c/G)^{1/2} \approx 1.22 \times 10^{19} \text{ GeV}/c^2$, where $s_k \in \{-1, 0, 1\}$. Since we observe photons of energy well below the Planck scale, the dominant LIV term is associated with the lowest order non-zero term in the sum, of order $n = \min\{k | s_k \neq 0\}$, which is usually assumed to be either linear ($n = 1$) or quadratic ($n = 2$). The photon propagation speed is given by the corresponding group velocity,

$$v_{\text{ph}} = \frac{\partial E_{\text{ph}}}{\partial p_{\text{ph}}} \approx c \left[1 - s_n \frac{n+1}{2} \left(\frac{E_{\text{ph}}}{M_{\text{QG},n} c^2} \right)^n \right]. \quad (2)$$

Note that $s_n = 1$ corresponds to the sub-luminal case ($v_{\text{ph}} < c$ and a positive time delay), while $s_n = -1$ corresponds to the super-luminal case ($v_{\text{ph}} > c$ and a negative time delay). Taking into account cosmological effects [9], this induces a time delay (or lag) in the arrival of a high-energy photon of energy E_h , compared to a low-energy photon of energy E_l (emitted simultaneously at the same location), of

$$\Delta t = s_n \frac{(1+n)}{2H_0} \frac{(E_h^n - E_l^n)}{(M_{\text{QG},n} c^2)^n} \int_0^z \frac{(1+z')^n}{\sqrt{\Omega_m(1+z')^3 + \Omega_\Lambda}} dz'. \quad (3)$$

Here we concentrate on our results for a linear energy dependence ($n = 1$).

We have applied this formula to the highest energy photon detected in GRB 080916C, with an energy of $E_h = 13.22^{+0.70}_{-1.54}$ GeV, which arrived at $t = 16.54$ s after the GRB trigger (i.e. the onset of the $E_l \sim 0.1$ MeV emission). Since it is hard to associate the highest energy photon with a particular spike in the low-energy lightcurve, we have made the conservative assumption that it was emitted anytime after the GRB trigger, i.e. $\Delta t \leq t$, in order to obtain a limit for the sub-luminal case ($s_n = 1$): $M_{\text{QG},1} > 0.1M_{\text{Planck}}$. This was the strictest limit of its kind [7], at that time.

However, the next very bright LAT GRB, 090510, was short and had very narrow sharp spikes in its light curve (see Fig 2), thus enabling us to do even better [8]. Our main results for GRB 090510 are summarized in Table 2. The first 4 limits are based on a similar method as described above for GRB 080916C, using the highest energy photon, $E_h = 30.53^{+5.79}_{-2.56}$ GeV, and assuming that its emission time t_h was after the start of a relevant lower energy emission episode: $t_h > t_{\text{start}}$. These 4 limits correspond to different choices of t_{start} , which are shown by the vertical lines in Fig. 2. We conservatively used the low end of the 1σ confidence interval for the highest energy photon ($E_h = 28$ GeV) and for the redshift ($z = 0.900$). The most conservative assumption of this type is associating t_{start} with the onset of any detectable emission from GRB 090510, namely the start of the small precursor that GBM triggered on, leading to $\xi_1 = M_{\text{QG},1}/M_{\text{Planck}} > 1.19$. However, it is highly unlikely that the 31 GeV photon is indeed associated with the small precursor. It is much more likely associated with the main soft gamma-ray emission, leading to $\xi_1 > 3.42$. Moreover, for any reasonable emission spectrum, the emission of the 31 GeV photon would be accompanied by the emission of a large number of lower energy photons, which would suffer a much smaller time delay due to LIV effects, and would therefore mark its emission time. We could easily detect such photons in energies above 100 MeV, and therefore the fact that significant high-energy emission is observed only at later times (see Fig. 2) strongly argues that the 31 GeV photon was not emitted before the onset of the observed high-energy emission. One could choose either the onset time of the emission above 100 MeV or above 1 GeV, which correspond to $\xi_1 > 5.12$, and $\xi_1 > 10.0$, respectively. ²

²We note that there is no evidence for LIV induced energy dispersion that might be expected if indeed the 31 GeV photon was emitted near our choices for t_{start} , together with lower energy photons, as can be expected for any reasonable emission spectrum. This is evident from the lack of accumulation of photons along the *solid* curves in panel (a) of Fig. 2, at least for the first 3 t_{start} values, and provides support for these choices of t_{start} (i.e. that they can indeed serve as upper limits on a LIV induced energy dispersion).

t_{start} (ms)	limit on $ \Delta t $ (ms)	Reason for choice of t_{start} or limit on Δt	E_l (MeV)	valid for s_n	lower limit on $M_{\text{QG},1}/M_{\text{Planck}}$
-30	< 859	start of any observed emission	0.1	1	> 1.19
530	< 299	start of main < 1 MeV emission	0.1	1	> 3.42
630	< 199	start of > 100 MeV emission	100	1	> 5.12
730	< 99	start of > 1 GeV emission	1000	1	> 10.0
—	< 10	association with < 1 MeV spike	0.1	± 1	> 102
—	< 19	if 0.75 GeV γ is from 1 st spike	0.1	± 1	> 1.33
$ \frac{\Delta t}{\Delta E} < 30 \frac{\text{ms}}{\text{GeV}}$		lag analysis of all LAT events	—	± 1	> 1.22

Table 2: Lower-limits on the Quantum Gravity (QG) mass scale associated with a possible linear ($n = 1$) variation of the speed of light with photon energy, that we can place from the lack of time delay (of sign s_n) in the arrival of high-energy photons relative to low-energy photons, from our observations of GRB 090510 (from [8]).

The 5th and 6th limits in Table 2 are more speculative, as they rely on the association of an individual high-energy photon with a particular spike in the low-energy light curve, on top of which it arrives. While these associations are not very secure (the chance probability is roughly $\sim 5 - 10\%$), they are still most likely, making the corresponding limits interesting, while keeping this big caveat in mind. The allowed emission time of these two high-energy photons, if these associations are real, is shown by the two thin vertical shaded regions in Fig. 2. For the 31 GeV photon this gives a limit of $\xi_1 > 102$ for either sign of s_n .

The last limit in Table 2 is based on a different method, which is complementary and constrains both signs of s_n . It relies on the highly variable high-energy light curve, with sharp narrow spikes, which would be smeared out if there was too much energy dispersion (of either sign). We have used the DisCan method [10] to search for linear energy dispersion within the LAT data (the actual energy range of the photons used was 35 MeV to 31 GeV)³ during the most intense emission interval (0.5–1.45 s). This approach extracts dispersion information from all detected LAT photons and does not involve binning in time or energy. Using this method we obtained a robust lower limit of $\xi_1 > 1.22$ (at the 99% confidence level).

Our most conservative limits (the first and last limits in Table 2) rely on very different and largely independent analysis, yet still give a very similar limit: $M_{\text{QG},1} > 1.2M_{\text{Planck}}$. This lends considerable support to this result, and makes it more robust and secure than for each of the methods separately.

³We obtain similar results even if we use only photons below 3 GeV or 1 GeV.

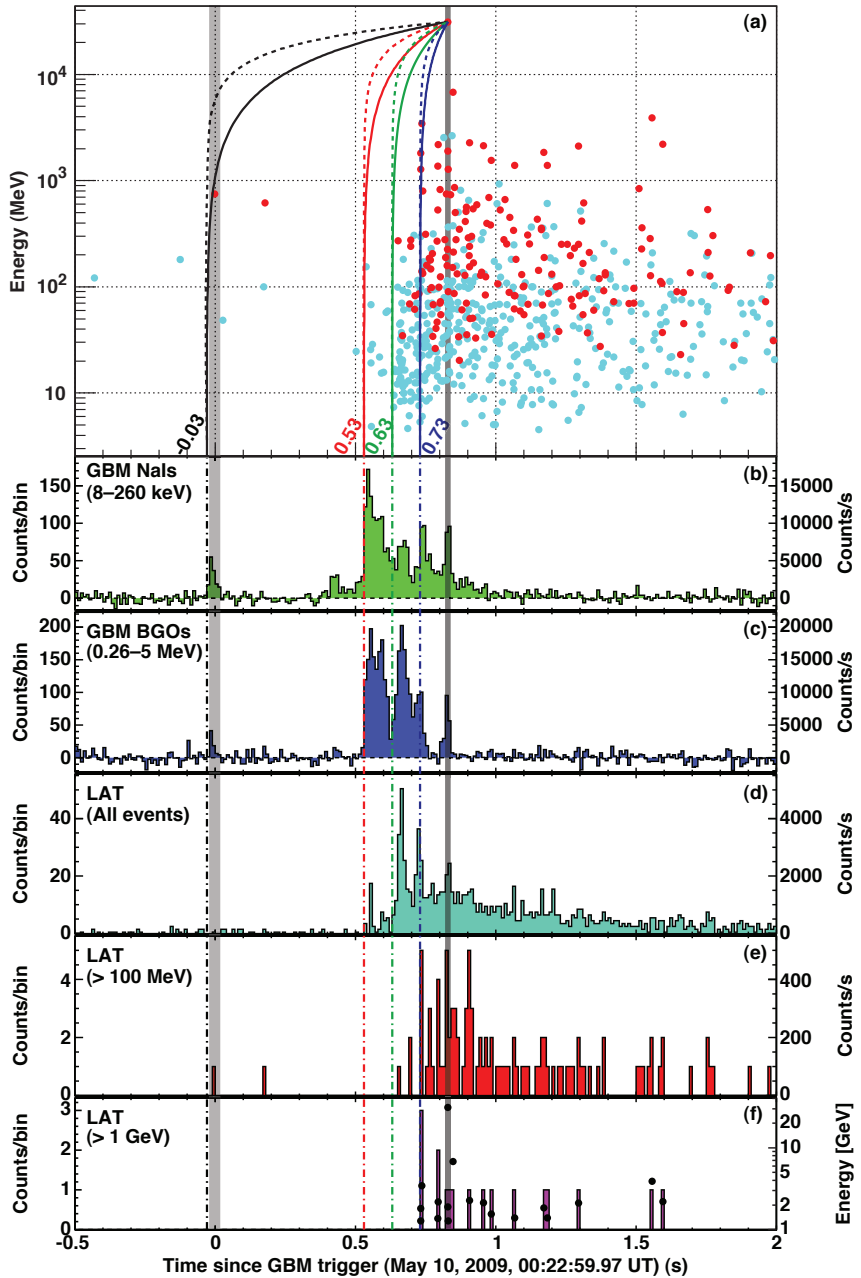


Figure 2: Light curves of GRB 090510 at different energies (for details see [8]).

4 Lower limits on the bulk Lorentz factor

The GRB prompt emission typically has very large isotropic equivalent luminosities ($L \sim 10^{50} - 10^{53} \text{ erg s}^{-1}$), significant short time scale variability, and typical photon energies $\gtrsim m_e c^2$ (in the source cosmological frame). This would result in a huge optical depth to pair production ($\gamma\gamma \rightarrow e^+e^-$) at the source, which would thermalize the spectrum and thus be at odds with the observed non-thermal spectrum, unless the emitting material was moving toward us relativistically, with a bulk Lorentz factor $\Gamma \gg 1$. This “compactness” argument has been used to derive lower-limits, Γ_{\min} , on the value of Γ , which were typically $\sim 10^2$ and in some cases as high as a few hundred (see [11] and references therein). However, the photons that provided the opacity for these limits were well above the observed energy range, so there was no direct evidence that they actually existed in the first place.

With Fermi, however, we adopt a more conservative approach of relying only on photons within the observed energy range. Under this approach,

$$\Gamma_{\min} \lesssim (1+z) \frac{E_{\text{ph,max}}}{m_e c^2} \approx 200(1+z) \left(\frac{E_{\text{ph,max}}}{100 \text{ MeV}} \right), \quad (4)$$

where $E_{\text{ph,max}}$ is the highest observed photon energy, so that setting a large Γ_{\min} requires observing sufficiently high-energy photons.

The main uncertainty in deriving Γ_{\min} is usually the exact choice for the variability time, t_v . Other uncertainties arise from those on the spectral fit parameters, or on the degree of space-time overlap between the high-energy photon and lower energy target photons, in cases where there is more than one spectral component without conclusive temporal correlation between their respective light curves. Finally, the fact that our limits rely on a single high-energy photon also induces an uncertainty, as it might still escape from an optical depth of up to a few. However, in most cases the second or third highest-energy photons help to relax the affect this has on Γ_{\min} (as the probability that multiple photons escape from $\tau_{\gamma\gamma} > 1$ rapidly decreases with the number of photons). Thus, we have derived reasonably conservative Γ_{\min} values for 3 of the brightest LAT GRBs: $\Gamma_{\min} \approx 900$ for GRB 080916C [7], $\Gamma_{\min} \approx 1200$ for GRB 090510 [12], and $\Gamma_{\min} \approx 1000$ for GRB 090902B [13]. This shows that short GRBs (such as 090510) are as highly relativistic as long GRBs (such as 080916C or 090902B), which was questioned before the launch of Fermi [14]. Since our highest values of Γ_{\min} are derived for the brightest LAT GRBs, they are susceptible to strong selection effects. It might be that GRBs with higher Γ tend to be brighter in the LAT energy range (e.g. by avoiding intrinsic pair production [15]).

5 Delayed onset and a distinct high-energy spectral component

A delayed onset of the high-energy emission (> 100 MeV) relative to the low-energy emission ($\lesssim 1$ MeV) appears to be a very common feature in LAT GRBs. It clearly appears in all 4 of the particularly bright LAT GRBs, while in dimmer LAT GRBs it is often inconclusive due to poor photon statistics near the onset time. The time delay, t_{delay} , appears to scale with the duration of the GRB ($t_{\text{delay}} \sim$ several seconds in the long GRBs 080916C and 090902B, while $t_{\text{delay}} \sim 0.1 - 0.2$ s in the short GRBs 090510 and 081024B, though with a smaller significance for the latter).

Only 3 LAT GRBs so far have shown clear ($> 5\sigma$) evidence for a distinct spectral component. However, these GRBs are the 3 brightest in the LAT, while the next brightest GRB in the LAT (080916C) showed a hint for an excess at high energies. This suggests that such a distinct high-energy spectral component is probably very common, but we can clearly detect it with high significance only in particularly bright LAT GRBs, since a large number of LAT photons is needed in order to detect it with $> 5\sigma$ significance.

The distinct spectral component is usually well fit by a hard power-law that dominates at high energies. In GRB 090902B a single power-law component dominates over the usual Band component both at high energies (above ~ 100 MeV) and low energies (below ~ 50 KeV; see *lower panel* of Fig. 3). There is also marginal evidence that the high-energy power-law component in GRB 090510, which dominates above ~ 100 MeV, might also appear at the lowest energies (below a few tens of keV).

Both the delayed onset and distinct spectral component relate to and may help elucidate the uncertain prompt GRB emission mechanism. The main two competing classes of models are leptonic and hadronic origin.

Leptonic: the high-energy spectral component might be inverse-Compton emission, and in particular synchrotron-self Compton (SSC) if the usual Band component is synchrotron. In this case, however, it may be hard to produce the observed $t_{\text{delay}} > t_v$, where t_v is the width of individual spikes in the lightcurve ($t_{\text{delay}} \lesssim t_v$ might occur due to the build-up of the seed synchrotron photon field in the emitting region over the dynamical time). Moreover, the gradual increase in the photon index β of the distinct high-energy power-law spectral component is not naturally expected in such a model, and the fact that it is different than the Band low-energy photon index as well as the excess flux (above the Band component) at low energies are hard to account for in this type of model.

Hadronic: t_{delay} might be identified with the acceleration time, t_{acc} , of protons (or heavier ions) to very high energies (at which they lose much of their energy on a dynamical time, e.g. via proton synchrotron [16], in order to have a reasonable radiative efficiency). If the observed high-energy emission (and in particular the distinct high-energy spectral component) also involves pair cascades (e.g. inverse-Compton emission by secondary e^\pm pairs [17] produced in cascades initiated by photo-hadronic interactions) then it might take some additional time for such cascades to develop. Such an origin for t_{delay} ($\sim t_{\text{acc}}$), however, requires the high-energy emission to originate from the same physical region over times $> t_{\text{delay}}$, and implies high-energy emission rise and variability times $t_v \gtrsim t_{\text{acc}} \sim t_{\text{delay}}$, due to the stochastic nature of the acceleration process (while $t_v < t_{\text{delay}}$ is usually observed). The gradual increase in β is not naturally expected in hadronic models, though it might be mimicked by a time-evolution of a high-energy Band-like spectral component [16]. For GRB 090510 a hadronic model requires a total isotropic equivalent energy $> 10^2$ times larger than that observed in gamma-rays [17], which may pose a serious challenge for the progenitor of this short GRB. The excess flux at low energies that is observed in GRB 090902B (and the hint for such an excess in GRB 090510) may be naturally explained in this type of model by synchrotron emission from secondary pairs [17, 13].

Altogether, hadronic models seem to fare somewhat better, however both leptonic and hadronic models still face many challenges, and do not yet naturally account for all of the Fermi observations.

6 Long-lived high-energy emission

In most LAT GRBs the high-energy (> 100 MeV) emission lasts significantly longer than the low-energy ($\lesssim 1$ MeV) emission. While the high-energy emission usually shows significant variability during the prompt (low-energy) emission phase, in some cases showing temporal correlation with the low-energy emission, the longer lived emission is typically temporally smooth and consistent with a power-law flux decay (of $\sim t^{-1.2} - t^{-1.5}$) with a LAT photon index corresponding to a roughly flat νF_ν .

It is most natural to interpret the prompt high-energy emission as the high-energy counterpart of the prompt soft gamma-ray emission, from the same emission region, especially when there is temporal correlation between the low and high-energy light curves, and sometimes even from the same spectral component (as appears to be the case for GRB 080916C). However, when there is no such temporal correlation, an origin from a different emis-

sion region is possible. The longer lived smooth power-law decay phase is more naturally attributed to the high-energy afterglow, from the forward shock that is driven into the external medium. An afterglow origin has been suggested in some cases for the whole LAT emission [20, 15], including during the prompt soft gamma-ray emission stage, however in this scenario it is generally hard to explain the sharp spikes in the LAT lightcurve during the prompt phase. It is easier to test the origin of this long lived high-energy emission when there is good multi-wavelength coverage of the early afterglow emission (e.g., in X-ray and/or optical), such as for GRB 090510 [18]. Producing particularly high-energy photons is challenging for a synchrotron origin, both during the prompt emission [7], and even more so during the afterglow (e.g. [21]), as it requires a very high bulk Lorentz factor and upstream magnetic field, in addition to a very efficient shock acceleration (e.g. a 33 GeV photon observed in GRB 090902B after 82 s, well after the end of the prompt emission [13], requires $\Gamma > 1500$).

7 High-energy emission of long versus short GRBs

So far, 2 (12) out of the 14 LAT GRBs are of the short (long) duration class. This implies that $\sim 14\%$ of LAT GRBs are short, with a large uncertainty due to the small number statistics, which is consistent with the $\sim 20\%$ short GRBs detected by the GBM. As can be seen from Table 1, the high-energy emission properties of short and long GRBs appear to be rather similar. They can both produce very bright emission in the LAT energy range (090510 vs. 080916C, 090902B and 090926), with a correspondingly high lower-limit on the bulk Lorentz factor ($\Gamma_{\min} \sim 10^3$), as well a distinct spectral component (090510 vs. 090902B and 090926). Both show a delayed onset and longer lived high-energy emission, compared to the low-energy emission. However, the delay in the onset of the high-energy emission appears to roughly scale with the duration of the GRB, being $\sim 0.1 - 0.2$ s for short GRBs and several seconds for long GRBs. This is especially intriguing when comparing GRBs 080916C and 090510, which had a comparable isotropic equivalent luminosity (of several 10^{53} erg s^{-1}), suggesting another underlying cause for the difference in the time delay (e.g. [22]).

Another interesting potential difference, which still needs to be confirmed (as there are only 2 short LAT GRBs so far, and possible selection effects), is that short GRBs appear to have a comparable energy output at high and low photon energies, while long GRBs tend to radiate a smaller fraction of their energy output at high photon energies (see *upper panel* of Fig. 3).

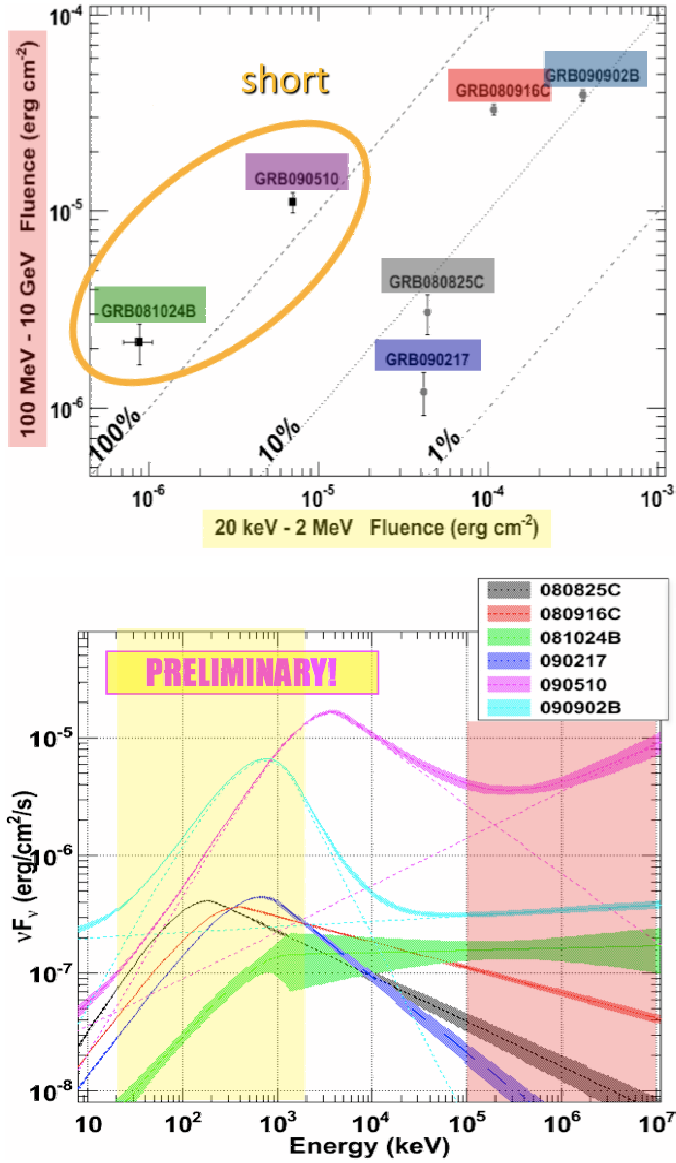


Figure 3: **Top panel:** the fluence at high (0.1–10 GeV) versus low (20 keV – 2 MeV) energies (from [19]), for 4 long (080825C, 080916C, 090217, 090902B) and 2 short (081024B, 090510) duration LAT GRBs. The diagonal lines indicate high to low energy fluence ratios of 1%, 10%, and 100%. **Bottom panel:** the best fit time-integrated νF_ν spectra for the same GRBs, two of which (090510, 090902B) show a distinct spectral component, well described by a hard power-law, in addition to the usual Band spectral component. The colored shaded regions indicate the energy ranges used for calculating the fluences that are displayed in the *top panel*.

JG gratefully acknowledges a Royal Society Wolfson Research Merit Award.

References

- [1] Hurley, K., *et al.* 1994, *Nature*, 372, 652
- [2] González, M. M., *et al.* 2003, *Nature*, 424, 749
- [3] Granot, J., & Guetta, D. 2003, *ApJ*, 598, L11
- [4] Pe'er, A. A., & Waxman, E. 2004, *ApJ*, 613, 448
- [5] Giuliani, A., *et al.* 2008, *A&A*, 491, L25
- [6] Band, D. L. , *et al.* 2009, *ApJ*, 701, 1673
- [7] Abdo, A. A., *et al.*, 2009, *Science*, 323, 1688
- [8] Abdo, A. A., *et al.*, 2009, *Nature*, 462, 331
- [9] Jacob, U., & Piran, T. 2008, *JCAP*, 01, 031
- [10] Scargle, J. D., Norris, J. P., & Bonnell, J. T. 2008, *ApJ*, 673, 972
- [11] Lithwick, Y., & Sari, R. 2001, *ApJ*, 555, 540
- [12] Abdo, A. A., *et al.*, 2010, submitted to *ApJ*
- [13] Abdo, A. A., *et al.*, 2009, 706, L138
- [14] Nakar, E. 2007, *Phys. Rep.*, 442, 166
- [15] Ghisellini, G., Ghirlanda, G., Nava, L., & Celotti, A. 2010, *MNRAS* in press (doi:10.1111/j.1365-2966.2009.16171.x; arXiv:0910.2459)
- [16] Razzaque, S., Dermer, C. D., & Finke, J. D. 2009, preprint (arXiv0908.0513)
- [17] Asano, K., Guiriec, S., & Mészáros, P. 2009, *ApJ*, 705, L191
- [18] De Pasquale, M., *et al.* 2010, *ApJ*, 709, L146
- [19] Abdo, A. A., *et al.* 2010, *ApJ* in press (arXiv:1002.3205)
- [20] Kumar, P., & Barniol Duran, R. 2009, *MNRAS*, 400, L75
- [21] Li, Z., & Waxman, E. 2006, *ApJ*, 651, 328
- [22] Toma, K., Wu, X. F., & Meszaros, P., 2010, preprint (arXiv:1002.2634)